# Absolute cross sections for the $^{61}$Ni($^{16}$O, $X$) reactions

J. C. Wells, Jr.*
*Tennessee Technological University, Cookeville, Tennessee 38501*

R. L. Robinson, H. J. Kim, and J. L. C. Ford, Jr.
*Oak Ridge National Laboratory,† Oak Ridge, Tennessee 37830*

(Received 1 July 1974)

The absolute cross sections for a number of different reactions resulting from the bombardment of $^{61}$Ni with 38.5, 41.0, 43.5, 46.0, 48.5, and 51.0 MeV $^{16}$O ions were determined from $\gamma$-ray yields observed from the decay of resulting radioactivities, and from yields of in-beam $\gamma$ rays. The total cross section was compared to an optical-model calculation. The relative population of the reaction products was compared to calculations for the statistical decay of a compound nucleus by $n$, $p$, and $\alpha$ evaporation. This model does account for the general features of the experimental results, and agrees reasonably well with the stronger exit channels.

[NUCLEAR REACTIONS: $^{61}$Ni($^{16}$O, $X$), $E_{^{16}O}$ = 38.5, 41.0, 43.5, 46.0, 48.5, and 51.0 MeV; measured $E_\gamma$, $I_\gamma$; deduced $\sigma(E)$.]

## I. INTRODUCTION

Heavy-ion bombardments are known to produce a variety of reaction products including some very neutron deficient nuclei which have not been produced in any other way. It is anticipated that increased heavy-ion projectile energies will permit studies still farther from the valley of $\beta$ stability. Efforts have been made to predict these cross sections but the calculations depend on physical phenomena which are not adequately understood, e.g., the reaction mechanism; the competition between particle emission, $\gamma$-ray decay, and fission; the level density dependence on spin; and the energy dependence of the yrast level. To provide experimental results by which these calculations could be tested, and implicitly the assumptions made in these calculations, we initiated a program to determine absolute cross sections for heavy-ion induced reactions with emphasis being placed on obtaining the cross sections for as many channels as possible. Intuitively, we believed that the channels with weaker cross sections would prove a more sensitive test of the calculations and of their ability to predict the very weak cross sections attributed to production of nuclei far from the valley of $\beta$ stability.

Results for $^{58,60}$Ni($^{16}$O, $X$) reactions were reported previously.[1] The cross sections were extracted from yields of $\gamma$ rays from residual radioactivities and of in-beam $\gamma$ rays. Here we report the results for the $^{61}$Ni($^{16}$O, $X$) reaction. Our rationale for continuing in the same mass region is twofold: (1) For a given isotope, some reaction channels are difficult to observe (e.g., extremely long lifetimes resulting in low yields, or large amounts of feeding from the decay of other radionuclides), while they may be observed easily with another isotope. As an example, the $^{60}$Ni($^{16}$O, 2$p$) channel is readily identified, but the $^{61}$Ni($^{16}$O, 2$p$)$^{75}$Se channel is not, due to the large production of $^{75}$Se via the $^{61}$Ni($^{16}$O, $pn$) reaction. (2) It is interesting to determine if some channels are consistently different from those predicted.

In this work, absolute cross sections for the $^{61}$Ni($^{16}$O, $X$) reactions were determined and their total cross section compared to the formation cross section calculated with an optical model, and the relative production of residual nuclei compared to calculations for statistical evaporation from a compound nucleus. Upper limits have been determined for cross sections for which more information is not available. Although the principal interest is in few-nucleon emission, for completeness we also looked for nuclei resulting from one or two particle transfer reactions.

## II. EXPERIMENTAL PROCEDURE

Targets of $^{61}$Ni were irradiated with 38.5, 41.0, 43.5, 46.0, 48.5, and 51.0 MeV $^{16}$O projectiles from the ORNL tandem Van de Graaff accelerator. A target of 92.4% enriched $^{61}$Ni, whose thickness was 0.99 mg/cm$^2$, was used for the activation measurements. This was backed by a 7 mg/cm$^2$ gold foil to stop the recoil products. A thick target of 74.4% enriched $^{61}$Ni, which completely stopped the beam, was used for the in-beam spectroscopy measurements.

The experimental setup was as follows: The

TABLE I. Experimental yields for the $^{61}$Ni($^{16}$O,$X$) reactions.

| $X$ | $E_{^{16}O}$(MeV) = 38.5 | 41.0 | 43.5 | 46.0 | 48.5 | 51.0 |
|---|---|---|---|---|---|---|
| | Reactions per incident $^{16}$O ion ($\times 10^{-8}$) | | | | | |
| $n$ | 0.15 ± 0.06 | <0.12 | 0.3 ± 0.2 | <0.8 | <2 | 5 ± 3 |
| $p$ | 0.06 ± 0.02 | 0.27 ± 0.09 | <0.3 | <0.5 | <6 | <0.5 |
| $2n$ | (0.39 ± 0.04)/$f$ | (2.7 ± 0.4)/$f$ | (6.3 ± 1.0)/$f$ | (8 ± 1)/$f$ | (12 ± 2)/$f$ | (7.4 ± 0.9)/$f$ |
| $2n$ } $pn$ } | 5.0 ± 0.4 | 29 ± 3 | 84 ± 10 | 106 ± 13 | 149 ± 16 | 115 ± 12 |
| $2p$ [a] | (0.13 ± 0.13)/$f$ | <0.4/$f$ | <4/$f$ | (58 ± 13)/$f$ | (34 ± 12)/$f$ | (41 ± 8)/$f$ |
| $3n$ [a] | <0.02 | <0.15 | <0.6 | 2.6 ± 1.6 | 11 ± 4 | 31 ± 4 |
| $p2n$ | <0.06 | <0.34 | <1.7 | 5 ± 3 | 22 ± 5 | 32 ± 6 |
| $2pn$ [a] | <0.2 | 3.3 ± 1.8 | 23 ± 7 | 81 ± 17 | 166 ± 30 | 306 ± 53 |
| $3p$ | <0.15 | 1.2 ± 0.8 | 2.0 ± 1.0 | 4.0 ± 1.8 | | 10.1 ± 3.4 |
| $\alpha$ | 0.05 ± 0.01 | 0.08 ± 0.04 | 0.11 ± 0.14 | <0.4 | 1.2 ± 1.0 | <1.0 |
| $\alpha n$ [a] | 0.38 ± 0.11 | 3.5 ± 0.5 | 15.8 ± 2.4 | 31 ± 5 | 76 ± 11 | 101 ± 15 |
| $\alpha p$ | 0.41 ± 0.04 | 3.6 ± 0.4 | 11 ± 1 | 19 ± 2 | 57 ± 17 | 37 ± 4 |
| $\alpha 2n$ | <0.01 | <0.03 | <0.05 | <0.08 | <0.5 | <0.1 |
| $\alpha pn$ | <0.01 | <0.1 | 1.5 ± 0.4 | 3.5 ± 0.9 | <6 | 30 ± 4 |
| $2\alpha$ | <0.02 | 0.35 ± 0.06 | 1.4 ± 0.3 | 1.7 ± 0.2 | <3 | 6.2 ± 0.9 |
| $^{12}$C [a] | | (0.38 ± 0.07)/$f$ | (1.3 ± 0.3)/$f$ | (2.2 ± 0.5)/$f$ | (4.9 ± 1.6)/$f$ | (7.8 ± 1.3)/$f$ |
| $^{14}$N [a] | <0.16/$f$ | <0.09/$f$ | <0.21/$f$ | <0.5/$f$ | <0.9/$f$ | <0.9/$f$ |
| $^{15}$N [a] | <0.19/$f$ | <0.08/$f$ | <0.19/$f$ | <0.5/$f$ | <0.8/$f$ | (1.1 ± 0.5)/$f$ |
| $^{15}$O [a] | <0.4 | <0.17 | <0.4 | <0.8 | <1.6 | <3.2 |

[a] These are reactions for which a thick target was used, which completely stopped the beam. For the other reactions, the $^{16}$O energy loss in the target was ~4 MeV.

beam was on target for a predetermined time. At the end of the irradiation time, the beam was stopped and the target moved to the detector position. A 16 384 channel analyzer was started, and a series of sequential 2048 channel spectra was taken with a Ge(Li) detector. At the end of the detection period the target was returned to the beam position and the cycle repeated. In addition, a record of the beam current was kept by storing current integrator pulses in a second analyzer as a function of time. For irradiations of more than an hour, the target was removed from the chamber after irradiation and taken to a lower background area for $\gamma$-ray detection.

Identification of the $\gamma$ rays from the radioactive products was based on their energies and relative intensities, and on the half-lives associated with their decay in intensity.

The irradiation and detection times were chosen to emphasize nuclei of particular lifetimes (see Ref. 1). In the present work, a bombarding time of 2000 sec followed by six 320-sec spectra was used to look for radiation products with half-lives from a few seconds to an hour, and a bombarding time of several hours followed by seven 1-h spectra was used to look for longer lived products.

$\gamma$-ray spectra were also taken with the target in-beam using a Ge(Li) detector to observe stable

TABLE II. Products of the $^{61}$Ni($^{16}$O,$X$)$Y$ reactions. For each reaction product is given the technique used ($A$ = activation, $I$ = in-beam), the $\gamma$-ray transition used to obtain the cross section, the nucleus in which the transition occurs, and the ratio $f$ of this $\gamma$ ray intensity to the total intensity.

| $X$ | $Y$ | Method | $E_\gamma$ (keV) | (Nucleus) | $f$ |
|---|---|---|---|---|---|
| $n$ | $^{76}$Kr | A | 315.7 | $^{76}$Br | 0.36 ± 0.02 |
| $p$ | $^{76}$Br | A | 559.5 | $^{76}$Se | 0.71 ± 0.04 |
| $2n$ | $^{75}$Kr | A | 132.4 | $^{75}$Br | Unknown |
| $2n$ } $pn$ } | $^{75}$Kr } $^{75}$Br } | A | 286.5 | $^{75}$Se | 0.91 ± 0.05 |
| $2p$ | $^{75}$Se | I | 286.5 | $^{75}$Se | Unknown |
| $3n$ | $^{74}$Kr | I | 429 | $^{74}$Kr | 0.90 ± 0.10 |
| $p2n$ | $^{74}$Br | A | 634.6 | $^{74}$Se | 0.98 ± 0.10 |
| $2pn$ | $^{74}$Se | I | 634.6 | $^{74}$Se | 0.90 ± 0.10 |
| $3p$ | $^{74}$As | A | 596.0 | $^{74}$Ge | 0.58 ± 0.03 |
| $\alpha$ | $^{73}$Se | A | 360.9 | $^{73}$As | 0.97 ± 0.05 |
| $\alpha n$ | $^{72}$Se | I | 862 | $^{72}$Se | 0.90 ± 0.10 |
| $\alpha p$ | $^{72}$As | A | 834.0 | $^{72}$Ge | 0.77 ± 0.04 |
| $\alpha 2n$ | $^{71}$Se | A | 147.2 | $^{71}$As | 0.47 ± 0.02 |
| $\alpha pn$ | $^{71}$As | A | 174.9 | $^{71}$Ge | 0.90 ± 0.05 |
| $2\alpha$ | $^{69}$Ge | A | 1106.4 | $^{69}$Ga | 0.28 ± 0.02 |
| $^{12}$C | $^{65}$Zn | I | 115.1 | $^{65}$Zn | Unknown |
| $^{14}$N | $^{63}$Cu | I | 670.4 | $^{63}$Cu | Unknown |
| $^{15}$N | $^{62}$Cu | I | 247.0 | $^{62}$Cu | Unknown |
| $^{15}$O | $^{62}$Ni | I | 1162.9 | $^{62}$Ni | 0.90 ± 0.10 |
| $^{17}$O | $^{60}$Ni | I | 1332.5 | $^{60}$Ni | 0.90 ± 0.10 |

reaction products. Identification in this case was by energy and intensity only.

### III. RESULTS

The method of obtaining cross sections is discussed in detail in Ref. 1. Our results are summarized in Table I. In this table is given the experimental yield per $^{16}$O projectile for each reaction. The absolute efficiency of the Ge(Li) detector for a given geometry was typically determined to ±8%. The target thickness was determined from weight and area measurements to an uncertainty of ±5%.

Table II shows, for each reaction $^{61}$Ni($^{16}$O, $X$)$Y$, the reaction products, the method used (activation or in-beam spectroscopy), the $\gamma$-ray transition used in the cross-section determination, the nucleus in which the transition occurs, and the ratio $f$ of the $\gamma$-ray intensity to the total intensity. For low energy $\gamma$ rays a correction was included for internal conversion. The ratio $f$ often did not have error assignments. In these cases, an assumed value of ±10% was used. For in-beam $\gamma$-ray studies, the cross sections were obtained from the $2^+ \rightarrow 0^+$ intensity in the even mass cases by assuming an $f$ of 0.90 ± 0.10. Details of the evidence for assigning $\gamma$ rays to specific reaction products are given in Appendix A.

To correct for target thickness, curves were fitted visually to the experimental yields given in Table I. From these curves the cross sections corrected for target thickness were extracted. These cross sections, which were the principal goal of this work, are plotted in Fig. 1. Since these cross sections were determined from smooth curves, experimental points are not shown. However, error bars are given for each curve in Fig. 1, indicating the probable error for that cross section. The total probable error for the best cases is 11%. In some reactions the ratio $f$ was completely unknown. The dashed curves in Fig. 1 are

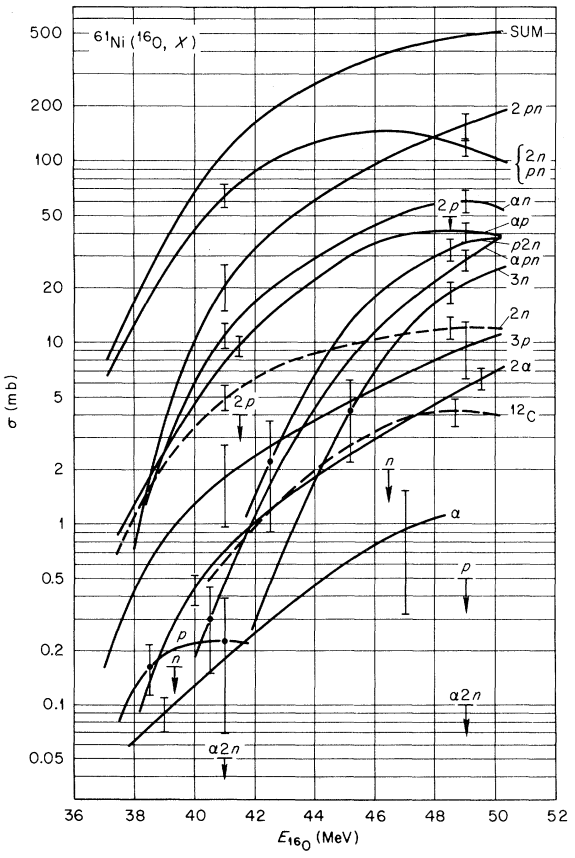


FIG. 1. Experimentally determined absolute cross sections for reaction products from $^{16}$O ions incident on $^{61}$Ni. Probable errors are indicated by the flags. The energies are in the laboratory system.

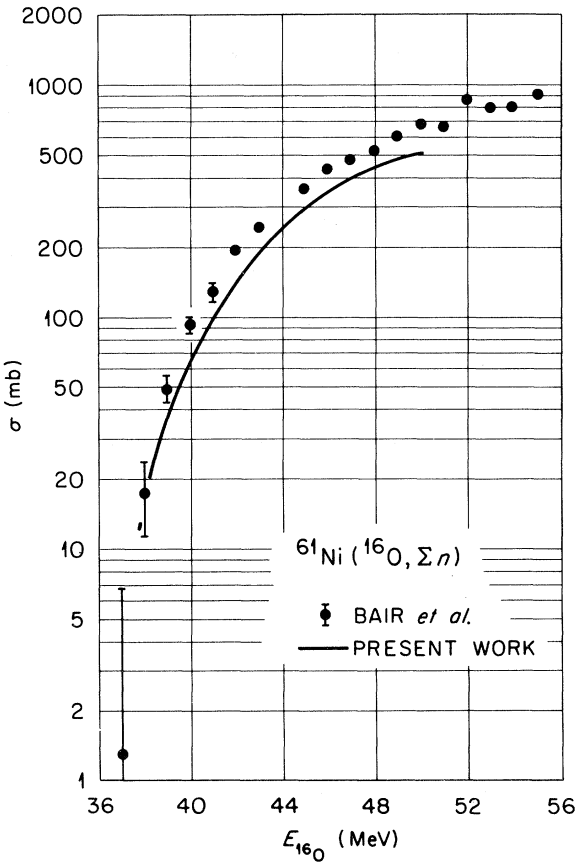


FIG. 2. Comparison of the cross sections for neutron emission obtained by Bair *et al.*[2] and in the present work for $^{16}$O irradiation of $^{61}$Ni. The uncertainty in our curve is ±11%.

for such reactions with $f$ set equal to 1.0 and represent, therefore, lower limits for the cross sections for these reactions. The curve labeled SUM is the sum of the cross sections actually observed.

The targets used for the activation measurements contained 5.3% $^{60}$Ni and 0.9% $^{62}$Ni, and the targets used for the in-beam measurements contained 15.6% $^{60}$Ni and 4.8% $^{62}$Ni. Corrections for reactions with these other isotopes were made by means of the published cross section results for $^{60}$Ni (Ref. 1) and some additional measurements made with a $^{62}$Ni target. The cross sections in Table I and the curves in Fig. 1 include these corrections.

As an independent check we have compared our results with some recent work of Bair *et al.*[2] They measured the total number of neutrons emitted in the Ni + $^{16}$O reactions as a function of projectile energy by means of a large graphite sphere with embedded $BF_3$ counters. Their results for the $^{61}$Ni target are shown in Fig. 2. The solid line gives the sum of our measured cross sections, each being multiplied by the number of neutrons emitted by the particular reaction.

Our results are lower by ~18% at the higher projectile energies. Their being lower is to be expected if any significant channels emitting neutrons are not included. The most important of these is probably the ($^{16}$O, 2$n$) reaction, which was not separated experimentally from the ($^{16}$O, $pn$) reaction. If the calculated ratio of the ($^{16}$O, 2$n$) cross section to the ($^{16}$O, $pn$) cross section is assumed to be approximately correct (see Sec. IV), and the ($^{16}$O, 2$n$) cross section based on this calculation is included, then the difference between our work and that of Bair *et al.* is reduced to ~13% at the higher projectile energies.

## IV. DISCUSSION

The cross sections for $^{61}$Ni($^{16}$O, $X$) are shown in Fig. 1. The curves all rise rapidly with projectile energy because of the Coulomb barrier. It is apparent that the total cross section is divided among a large number of exit channels, and that charged particle emission competes strongly with neutron emission. In Fig. 3, a comparison is made among the cross section results for $^{58}$Ni, $^{60}$Ni, and $^{61}$Ni (the first two from Ref. 1). This illustrates the degree to which proton emission decreases and neutron emission increases as the isotopic mass increases. This trend has been pointed out by Nolte *et al.*,[3] and is supported by the total neutron cross-section work of Bair *et al.*[2]

The sum of the experimental cross sections has been compared in Fig. 4 with the reaction cross section calculated with an optical model using the computer code GENOA developed by Perey.[4] We have used two sets of optical-model parameters which are appropriate for reactions between $^{16}$O and Ni. One is denoted as Set I by Christensen

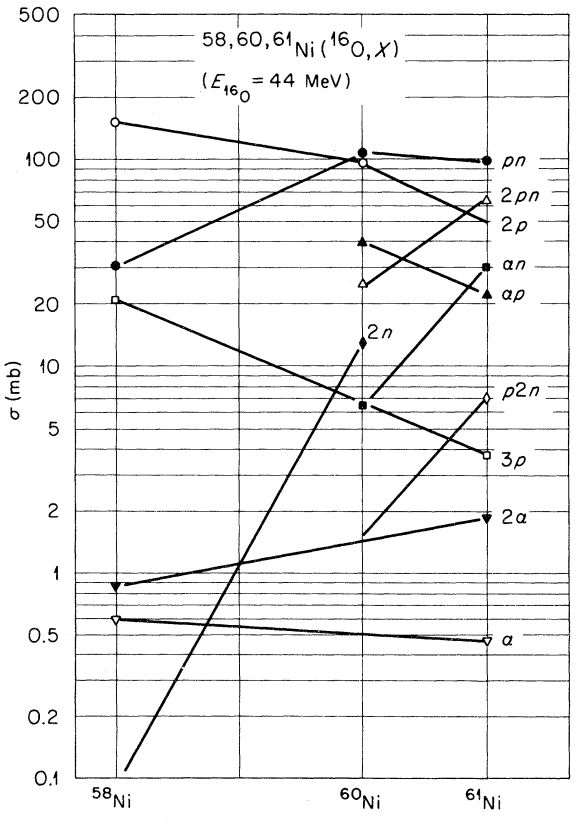


FIG. 3. Comparison of absolute cross sections as a function of isotopic mass for reaction products from $^{16}$O ions incident on $^{58,60,61}$Ni. The straight lines are to guide the eye. When no symbol appears at the end of a line, an upper limit is indicated.

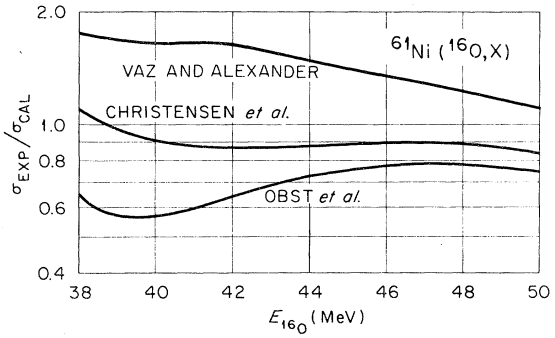


FIG. 4. Comparison of the sum of the experimental cross sections with the total reaction cross section calculated with the two sets of optical model parameters given in Refs. 5 and 6, and with the parabolic barrier potential parameters given in Ref. 7. The experimental uncertainty is ±11%.

*et al.* in Ref. 5, and the other is from Obst, McShan, and Davis.[6] According to the statistical model, the ($^{16}$O, $2p$) reaction was the only significant channel not experimentally observed. Its cross section was estimated from the statistical decay calculations to be 2–9% of the total cross section (see Fig. 5), and was added to the experimental sum in Fig. 1 in order to make a more valid comparison with optical-model predictions.

The experimental total cross section was also compared in Fig. 4 with calculations made by a procedure suggested by Vaz and Alexander.[7] They used a parabolic barrier potential which led to an expression for the reaction cross section[8]

$$\sigma_R = (\tfrac{1}{2}R_0^2)(\hbar\omega_0/E)\ln\{1+\exp[2\pi(E-E_0)/\hbar\omega_0]\} .$$

The cross section is averaged over barrier heights $E_0$ in the range $\bar{E}_0-\Delta$ to $\bar{E}_0+\Delta$. Parameters from their systematics appropriate for the $^{61}$Ni + $^{16}$O reaction are $R_0 = 9.16$ fm, $\bar{E}_0 = 32.5$ MeV, $\hbar\omega_0 = 4.0$ MeV, and $\Delta = 3.0$ MeV. Note in Fig. 4 that these systematics underestimate the reaction cross section, while the optical-model calculations tend to overestimate it.

We have calculated the relative population of the reaction products, assuming statistical decay of a compound nucleus, with the computer code ALICE developed by Blann and Plasil.[9] A comparison between our experimental results and the calculations is shown in Figs. 5 and 6. Both experimental and calculated results are given as the percent of total decay at each projectile energy. Binding energies used in the calculations came from mass excesses compiled by Wapstra and Gove.[10] The calculations include the dependence of the nuclear level density on spin. In addition, each emitted neutron, proton, and $\alpha$ particle carries off, respectively, 2, 3, and 10 units of angular momentum.

Many of the channels have cross sections in reasonable agreement with the calculated values. However, the experimental results for the $^{61}$Ni-

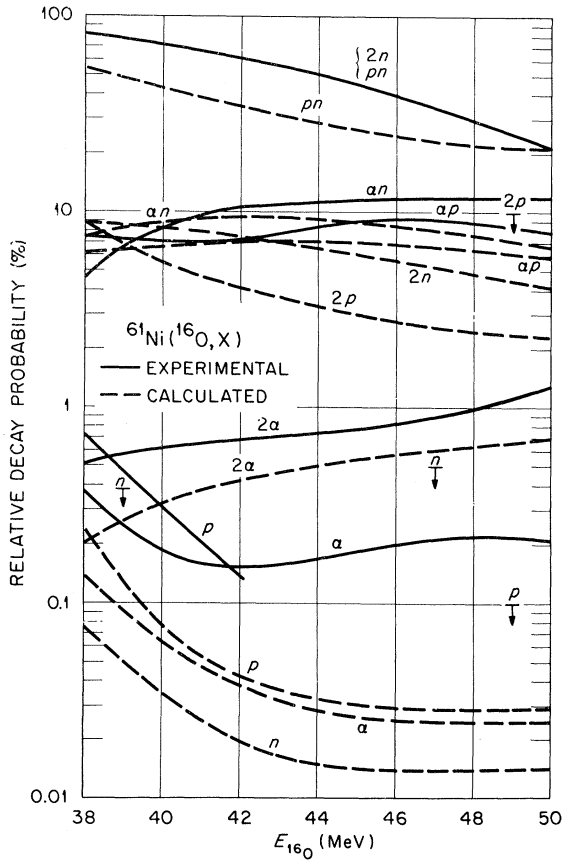


FIG. 5. Comparison of the relative probability of one and two particle emission as determined experimentally, and as calculated with a statistical evaporation model. The relative probability is in percent.

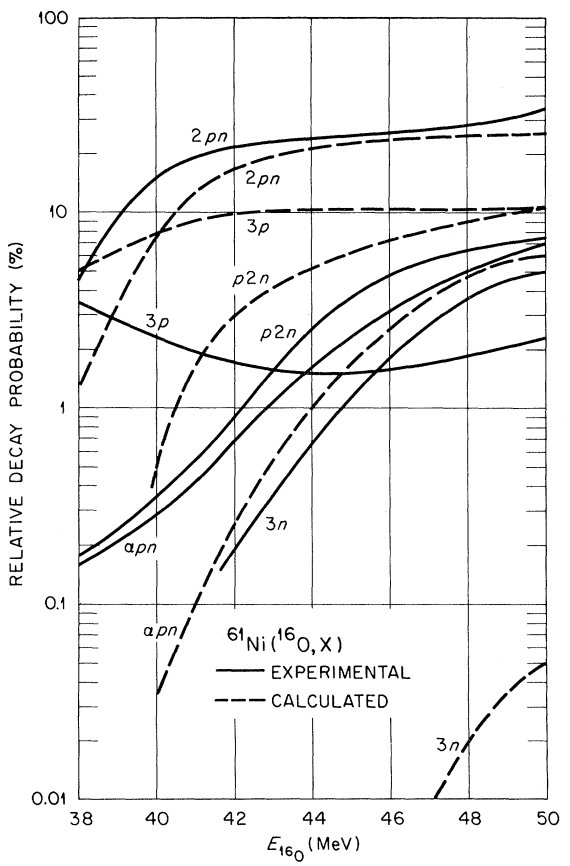


FIG. 6. Comparison of the relative probability of three particle emission as determined experimentally, and as calculated with a statistical evaporation model. The relative probability is in percent.

($^{16}$O, $3n$)$^{74}$Kr reaction, which leads to the nucleus farthest from stability, are two orders of magnitude larger than the calculations (see Fig. 6). This result, while significant in that it suggests that the cross sections for production of neutron deficient nuclei may be larger than present calculations indicate, is surprising since the $^{60}$Ni($^{16}$O, $2n$)-$^{74}$Kr reaction, which leads to the same residual nucleus, was in reasonable agreement with the calculations.[1]

Other channels whose cross sections differ significantly from the calculations are ($^{16}$O, $3p$), ($^{16}$O, $p$), and ($^{16}$O, $\alpha$). However, the latter two channels do have large experimental uncertainties.

The ($^{16}$O, $^{12}$C) and ($^{16}$O, $3\alpha$) reactions lead to the same reaction product. Since the calculated relative population for $3\alpha$ is $<0.1\%$, the ($^{16}$O, $^{12}$C) reaction is believed to predominate.

A possible cause of the differences between calculated relative population and experimental results may be the fact that $\gamma$-ray competition is not included in the code ALICE . As pointed out by Grover and Gilat,[11] $\gamma$-ray competition is not negligible, and is especially important for excitations within a particle binding energy of the yrast level. Other possible causes of the differences could be incorrect binding energies, variation of level density from one nucleus to another, and noncompound nuclear processes.

## APPENDIX A: EVIDENCE FOR IDENTIFICATION OF THE REACTION PRODUCTS

In this Appendix, evidence for the different reaction products is discussed. The degree of confidence for identifying a particular product depends on the extent of similarity between the $\gamma$-ray energies, intensities, and decay half-lives determined here and those previously reported. Column 4 in Table II gives the $\gamma$-ray transition used to obtain the cross section for each reaction.

The production of $^{76}$Kr + $n$ was based on the 315.7-keV $\gamma$ ray from the decay of $^{76}$Kr.[12] A $\gamma$ ray of the same energy was also produced by the decay of $^{75}$Br, which had one of the largest cross sections. Also, production of $^{76}$Kr from the $^{62}$Ni in the target was significant at the lower projectile energies. These contributions were subtracted from the total yield. As a consequence, the uncertainty of this cross section is large.

The production of $^{76}$Br + $p$ was based on the 559.5-keV $\gamma$ ray from the decay of $^{76}$Br.[13] Three other $\gamma$ rays which should be produced by this decay were not observed with the correct intensities and half-life. Production of $^{76}$Br from the $^{62}$Ni in the target caused large uncertainty in this cross section, and made possible only an upper limit determination for projectile energies above 42 MeV.

Evidence for the production of $^{75}$Kr + $2n$ was based on the 132.4-keV $\gamma$ ray from the decay of $^{75}$Kr.[14,15] The ratio $f$ of the decay of this $\gamma$ ray to the total decay was completely unknown, so only relative cross sections were obtained for this channel.

The sum of $^{75}$Kr + $2n$ and $^{75}$Br + $pn$ production was determined by the 286.5-keV $\gamma$ ray from the decay of $^{75}$Br.[16] Twenty-three other $\gamma$ rays were observed from this decay, and all had the correct intensities and half-life.

The production of $^{75}$Se + $2p$ was based on the $(\frac{3}{2}^-, \frac{5}{2}^-) \rightarrow \frac{5}{2}^+$ 286.5-keV $\gamma$ ray of $^{75}$Se observed in-beam.[16] A $\gamma$ ray of this energy was observed, but its yield as a function of projectile energy did not follow the pattern expected for a thick target. Thus, only upper limits for this reaction cross section could be obtained.

The production of $^{74}$Kr + $3n$ was based on the $2^+ \rightarrow 0^+$ 429-keV $\gamma$ ray and the $4^+ \rightarrow 2^+$ 674-keV $\gamma$ ray of $^{74}$Kr observed in-beam.[3] A correction for another 429-keV $\gamma$ ray produced in the $^{61}$Ni($^{16}$O, $2x$) reactions was applied. Production of $^{74}$Kr from the $^{60}$Ni in the target was significant at lower projectile energies. This contribution was also subtracted from the total yield. The cross sections determined separately with the 429-keV and 674-keV $\gamma$ rays agreed with each other within experimental error.

The production of $^{74}$Br + $p2n$ was determined by the 634.6-keV $\gamma$ ray from the decay of $^{74}$Br.[17] Eighteen other $\gamma$ rays were observed which were attributed to this decay, and all had the correct intensities and half-life. Production of $^{74}$Br from the $^{60}$Ni in the target was significant at lower projectile energies. Corrections were made for this contribution to the $^{74}$Br yield.

The production of $^{74}$Se + $2pn$ was determined by in-beam $\gamma$-ray spectroscopy of the $2^+ \rightarrow 0^+$ 634.6-keV $\gamma$ ray in $^{74}$Se.[17] Production of $^{74}$Se from the $^{60}$Ni in the target was significant at lower projectile energies. Corrections were made for this contribution to the $^{74}$Se yield.

The production of $^{74}$As + $3p$ was based on the 596.0-keV $\gamma$ ray from the decay of $^{74}$As.[18] A $\gamma$ ray of this energy was also produced by the decay of $^{75}$Br, which had one of the largest cross sections. The contribution from $^{75}$Br was subtracted from the total yield. As a consequence, the uncertainty in this cross section is large.

The production of $^{73}$Se + $\alpha$ was based on the 360.9-keV $\gamma$ ray from the decay of $^{73}$Se.[19] This $\gamma$ ray had the correct half-life. However, no other $\gamma$ rays were observed, so intensity comparisons could not be made. Production of $^{73}$Se from the

$^{60}$Ni and $^{62}$Ni in the target was especially significant at higher projectile energies. This contribution was subtracted from the total yield. As a consequence, the uncertainty in this cross section is large.

The production of $^{72}$As + $\alpha p$ was based on the 834.0-keV $\gamma$ ray from the decay of $^{72}$As.[20] Four other $\gamma$ rays were observed which could be attributed to this decay, and all had the correct intensities and half-life.

The production of $^{71}$Se + $\alpha 2n$ was based on the 147.2-keV $\gamma$ ray from the decay of $^{71}$Se.[21] This $\gamma$ ray was not observed in any spectra. From statistical fluctuations of the background radiation at this energy, upper limits for this reaction cross section were obtained.

The production of $^{71}$As + $\alpha pn$ was based on the 174.9-keV $\gamma$ ray from the decay of $^{71}$As with a half-life of 62 h.[22] Analysis of the yield curve of this $\gamma$ ray showed it to be a doublet with a short-lived component ($\tau_{1/2}$ = 1.3 h), which was dominant at low projectile energies and disappeared at higher projectile energies. A least-squares analysis was performed with the short half-life and both intensities as variable parameters, and the contribution to the production of $^{71}$As was determined. Production of $^{71}$As from the $^{60}$Ni in the target was significant at lower projectile energies. Corrections were made for this contribution to the $^{71}$As yield.

The production of $^{69}$Ge + 2$\alpha$ was based on the 1106.4-keV $\gamma$ ray from the decay of $^{69}$Ge.[23] This $\gamma$ ray had the correct half-life. No other $\gamma$ rays from this decay were observed, however, so intensity comparisons could not be made.

The production of $^{72}$Se + $\alpha n$, $^{65}$Zn + $^{12}$C, $^{63}$Cu + $^{14}$N, $^{62}$Cu + $^{15}$N, $^{62}$Ni + $^{15}$O, and $^{60}$Ni + $^{17}$O was based on the $\gamma$ rays and $f$ values shown in Table II, which were obtained from Ref. 24. In most of these cases, only upper limits were obtained. The $\gamma$ rays from $^{60}$Ni which might result from the $^{61}$Ni($^{16}$O, $^{17}$O) reaction could be completely accounted for by Coulomb excitation of the $^{60}$Ni in the target.

---

*Work supported in part by Oak Ridge Associated Universities.

†Research sponsored by the U.S. Atomic Energy Commission under contract with Union Carbide Corporation.

[1]R. L. Robinson, H. J. Kim, and J. L. C. Ford, Jr., Phys. Rev. C 9, 1402 (1974).

[2]J. K. Bair, W. B. Dress, C. H. Johnson, and P. H. Stelson, private communication; and Bull. Am. Phys. Soc. 17, 530 (1972).

[3]E. Nolte, W. Kutschera, Y. Shida, and H. Morinaga, Phys. Lett. 33B, 294 (1970).

[4]F. G. Perey, private communication.

[5]P. R. Christensen, I. Chernov, E. E. Gross, R. Stokstad, and F. Videbaek, Nucl. Phys. A207, 433 (1973).

[6]A. W. Obst, D. L. McShan, and R. H. Davis, Phys. Rev. C 6, 1814 (1972).

[7]L. C. Vaz and J. M. Alexander, Phys. Rev. C 10, 464 (1974).

[8]C. Y. Wong, Phys. Rev. Lett. 31, 766 (1973).

[9]M. Blann and F. Plasil, private communication; M. Blann, in *Proceedings of Heavy Ion Summer Study, Oak Ridge National Laboratory*, edited by S. T. Thornton (U.S. Atomic Energy Commission Technical Information Center, Oak Ridge, Tennessee, 1972), CONF 720669, p. 269; Phys. Rev. 157, 860 (1967).

[10]A. H. Wapstra and N. B. Gove, Nucl. Data A9, 267 (1971).

[11]J. R. Grover and J. Gilat, Phys. Rev. 157, 802 (1967).

[12]T. Paradellis, A. Houdayer, and S. K. Mark, Nucl. Phys. A201, 113 (1973).

[13]I. M. Ladenbauer-Bellis, H. Bakhru, and R. Bakhru, Can. J. Phys. 49, 54 (1971).

[14]P. G. Hansen *et al.* (ISOLDE collaboration), Phys. Lett. 28B, 415 (1969).

[15]Cary Davids, private communication.

[16]S. Ray, J. N. Mo, S. Muszynski, and S. K. Mark, Nucl. Phys. A138, 49 (1969).

[17]S. Göring and M. V. Hartrott, Nucl. Phys. A152, 241 (1970).

[18]J. R. Van Hise, and C. Paperiello, Nucl. Phys. A188, 148 (1972).

[19]R. D. Meeker and A. B. Tucker, Nucl. Phys. A157, 337 (1970).

[20]David C. Camp, Nucl. Phys. A121, 561 (1968).

[21]Ulrich Frhr. v. Hundelschausen, Z. Phys. 225, 125 (1969).

[22]G. Murray, N. E. Sanderson, J. C. Willmott, Nucl. Phys. A171, 435 (1971).

[23]W. H. Zoller, G. E. Gordon, and W. B. Walters, Nucl. Phys. A124, 15 (1969).

[24]*Nuclear level schemes A = 45 through A = 257 from Nuclear Data Sheets*, edited by the Nuclear Data Group, Oak Ridge National Laboratory (Academic, New York, 1973).